Currents and transports of the Monsoon Current south of Sri Lanka

F. Schott, J. Reppin, and J. Fischer
Institut für Meereskunde, Universität Kiel, Kiel, Germany

D. Quadfasel
Institut für Meereskunde, Universität Hamburg, Hamburg, Germany

Abstract. The zonal monsoon circulation south of India/Sri Lanka is a crucial link for the exchange between the northeastern and the northwestern Indian Ocean. The first direct measurements from moored stations and shipboard profiling on the seasonal and shorter-period variability of this flow are presented here. Of the three moorings deployed from January 1991 to February 1992 along 80°30'E between 4°11'N and 5°39'N, the outer two were equipped with upward looking acoustic Doppler current profilers (ADCPs) at 260-m depth. The moored and shipboard ADCP measurements revealed a very shallow structure of the near-surface flow, which was mostly confined to the top 100 m and required extrapolation of moored current shears toward the surface for transport calculations. During the winter monsoon, the westward flowing Northeast Monsoon Current (NMC) carried a mean transport of about 12 Sv in early 1991 and 10 Sv in early 1992. During the summer monsoon, transports in the eastward Southwest Monsoon Current (SMC) were about 8 Sv for the region north of 3°45'N, but the current might have extended further south, to 2°N, which would increase the total SMC transport to about 15 Sv. The circulation during the summer was sometimes found to be more complicated, with the SMC occasionally being separated from the Sri Lankan coast by a band of westward flowing low-salinity water originating in the Bay of Bengal. The annual-mean flow past Sri Lanka was weakly westward with a transport of only 2–3 Sv. Using seasonal-mean ship drift currents for surface values in the transport calculations yielded rather similar results to upward extrapolation of the moored profiles. The observations are compared with output of recent numerical models of the Indian Ocean circulation, which generally show the origin of the zonal flow past India/Sri Lanka to be at low latitudes and driven by the large-scale tropical wind field. Superimposed on this zonal circulation is local communication along the coast between the Bay of Bengal and the Arabian Sea.

1. Introduction

The circulation system in the Indian Ocean north of about 10°S undergoes drastic seasonal changes under the influence of the seasonally reversing monsoon wind system. During the winter monsoon, November to February, the Somali Current flows southward, carrying water from the Arabian Sea across the equator, where it merges with the northward flowing East African Coast Current at a latitude range of 2°–4°S to form the eastward flowing South Equatorial Counter Current. How much water is transferred across the Arabian Sea from south of the Indian peninsula to feed into the northern part of the Somali Current is not clear at the present time. Climatological surface current maps derived from historical ship drifts [*Cutler and Swallow*, 1984; *Rao et al.*, 1989] show a westward flow south of India/Sri Lanka during the winter monsoon, partly continuing westward at low latitudes, and partly branching toward the northwest into the Arabian Sea. This current is referred to here as the Northeast Monsoon Current (NMC). How it relates to the

overall circulation of the northern Indian Ocean is not well understood. While during the early part of the winter monsoon a well-established southward boundary current in the Bay of Bengal is detectable in the ship drifts, suggesting a linkage of both basins via the NMC, the source of the westward flow south of Sri Lanka in the later part of the winter appears to originate more to the east, in the same latitude belt. Surface water mass signatures south and west of Sri Lanka [e.g., *Wyrtki*, 1971] show a westward and northwestward spreading of low-salinity Bay of Bengal water in the winter monsoon, confirming the linkage function of the NMC. A similar linkage is also present in the numerical model studies reported by *McCreary et al.* [1993]. In their solution, the flow around the Indian subcontinent is generated by the propagation of baroclinic Kelvin waves.

During the summer monsoon, June to September, the Somali Current flows northward, feeding the "Great Whirl" between 5° and 10°N, and it has not yet been satisfactorily established how much of its transport just recirculates southward offshore and how much actually enters the interior Arabian Sea and is transferred eastward toward India. The ship drifts show the current south of India/Sri Lanka (Southwest Monsoon Current, SMC) to flow eastward during this
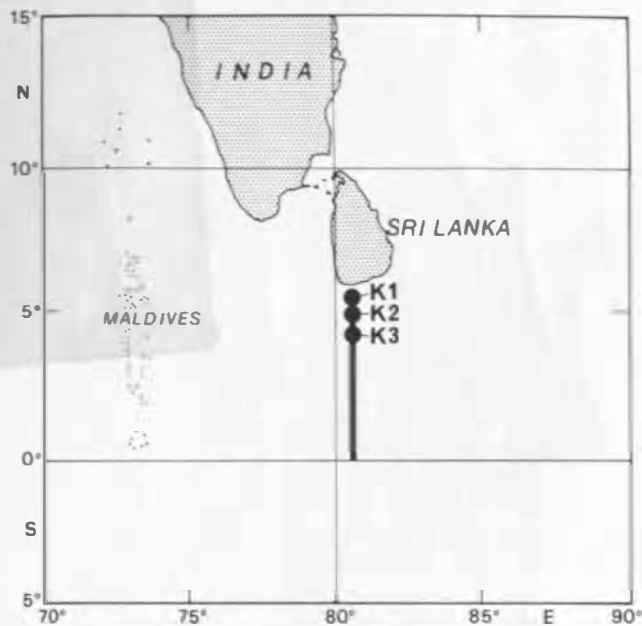
Figure 1a. Location of moored array south of Sri Lanka.

time period. The surface flow along the west coast of India is generally southward [e.g., *Shetye et al.*, 1990] during the summer monsoon, and the western boundary current in the Bay of Bengal is northward [*Cutler and Swallow*, 1984; *Rao et al.*, 1989], suggesting again that the Monsoon Current links both circulation systems during this period. On the other hand, in model realizations, the SMC seems to carry water from lower latitudes in the west of Sri Lanka eastward rather than being fed by a boundary current along the west coast of India [e.g., *Woodberry et al.*, 1989; *Semtner and Chervin*, 1992]. The surface salinity distribution [*Wyrtki*, 1971] shows propagation of higher-saline waters eastward south of Sri Lanka during this season which are originating in the west and offshore of India and clearly separated from the low-salinity waters of the Indian shelf and continental slope region.

In the transition periods between the monsoons, i.e., April–May and October–November, eastward winds over the equator drive the *Wyrtki* [1973] equatorial surface jet with velocities of 80 cm s^{-1} in the central Indian Ocean [*Reverdin*, 1987; *Rao et al.*, 1989]. This semiannual signal has effects on the seasonal cycle elsewhere in the tropical Indian Ocean, e.g., by forcing semiannual variability in the Somali Current through Rossby wave radiation [*Visbeck and Schott*, 1992] or circulation variability in the Bay of Bengal through Kelvin and Rossby wave radiation [*Potemra et al.*, 1991]. The semiannual currents in the equatorial belt of the central Indian Ocean decay significantly in the meridional direction [*Rao et al.*, 1989; *Visbeck and Schott*, 1992] but should still provide a nonnegligible contribution to the variability of the Monsoon Current.

Almost no measurements exist that describe the subsurface structure of the Monsoon Current. As observed by *Shetye et al.* [1990] during the summer monsoon, the subsurface flow underneath the southward surface flow off the west Indian coast was in the opposite direction, as is typical for an eastern boundary coastal upwelling regime. Whether

that undercurrent extended southward to Sri Lanka remained unknown.

A measurement program with moored current-meter stations and ship sections across the Monsoon Current (Figure 1a) was carried out as part of the World Ocean Circulation Experiment (WOCE) Indian Ocean program, beginning in December 1990 with the deployment of three moorings (Figure 1b), two of which carried upward looking acoustic Doppler current profilers (ADCPs). During the deployment cruise with R/V *Sonne*, measurements with shipboard ADCP, Pegasus current profiler and conductivity-temperature-depth (CTD)/sonde were carried out across that current. That survey showed low-salinity water with near-surface minimum values down to 32 psu near the coast of Sri Lanka, separated by a front near 4°15'N from the more saline Tropical Surface Water. The flow of this low-salinity water was westward and confined to the upper 100 m. The low salinity suggested the origin of this water to be the northern Bay of Bengal from where it is presumably carried to Sri Lanka via a southward western boundary current. The moorings were recovered during March 3–5, 1992, and thus covered the late winter monsoon phase of two consecutive years, 1991 and 1992. Only few shipboard measurements could be taken during the retrieval cruise because a harbor tug had to be used for lack of research vessel availability. These observations showed a similar situation of currents and stratification as in January 1991: low-surface salinities (34.0–34.4 psu) and westward near-surface flow. A later cruise in July 1993, again with R/V *Sonne*, showed eastward near-surface flow, commensurate with the summer monsoon
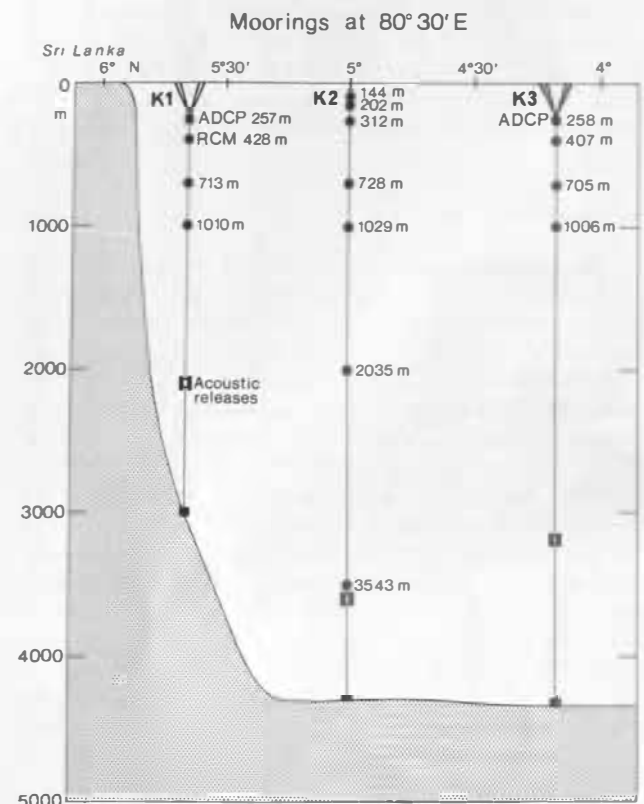

Figure 1b. Topography along 80°30'E and instrument distribution on moorings K1–K3.

Table 1. Means and Standard Deviations of Current-Meter Time Series

Mooring	Position	Water Depth, m	Deployment Period	Instrument Type	Record Depth, m	Annual (Jan. 12, 1991 to Jan. 12, 1992)		Fluctuating Kinetic Energy, cm^2 s^{-2}
						Means and Standard Deviations, cm s^{-1}		
						East Component	North Component	
K1	5°38.8′N, 80°31.0′E	3020	Dec. 28, 1990, to March 3, 1992	ADCP	75*	−17.3 ± 32.6*	4.0 ± 13.2*	619*
					100	−15.8 ± 22.8	2.7 ± 12.1	334
					200	−5.1 ± 17.2	1.5 ± 7.5	176
				RCM	428	3.3 ± 11.1	0.7 ± 3.7	69
				RCM	713	4.4 ± 12.5	2.0 ± 4.7	89
				RCM	1010	1.1 ± 8.2	0.6 ± 3.3	39
K2	5°00.2′N, 80°30.0′E	4295	Jan. 9, 1991, to March 3, 1992	RCM	144	−6.1 ± 12.6	−1.8 ± 9.6	125
				RCM	202	−0.5 ± 12.9	−0.3 ± 9.3	126
				RCM	312	3.3 ± 11.6	0.0 ± 8.5	104
				RCM	728	0.7 ± 6.1	0.5 ± 4.6	30
				RCM	1029	−0.6 ± 8.7	−0.4 ± 7.8	68
				RCM	2035	−1.2 ± 5.4	−0.3 ± 4.3	24
				RCM	3543	−0.2 ± 4.6	0.1 ± 3.6	17
K3	4°10.7′N, 80°29.5′E	4330	Jan. 8, 1991, to March 5, 1992	ADCP	30	0.3 ± 31.0	0.7 ± 16.0	609
					50	1.0 ± 26.9	2.0 ± 15.5	482
					100	−1.5 ± 16.2	−1.2 ± 12.4	208
					200	−0.6 ± 9.2	0.8 ± 9.1	83
				RCM	407	−2.0 ± 8.2	1.1 ± 6.4	55
				RCM	705	−0.3 ± 7.4	0.2 ± 4.9	40
				RCM	1006	1.2 ± 10.7	0.9 ± 7.7	86

*Gappy record.

situation. This flow occurred in a much broader latitudinal band than observed during the winter monsoon, and was separated from the Sri Lankan coast by a small belt of low-salinity westward flow.

This paper presents the results of the moored current measurements and derived transports and discusses seasonal developments of the circulation in relation to other evidence, e.g., from our own ship sections, from historical ship drift data and from numerical models. The focus here will be on the seasonal cycle of the near-surface flow. There is also a complex structure observed in the deep flow that may be part of oscillations in the equatorial wave guide and will be addressed elsewhere in conjunction with the evaluation of near-equatorial observations still in progress.

2. The Observations

The northernmost mooring was deployed on December 28 at 5°39′N, over 3000-m water depth on the steep continental slope (Figure 1). The spacing of the other two moorings was decided upon after the ship returned northward from its measurement program along 80°30′E that extended to 6°S. After the seaward edge of the boundary current was found near 4°15′N, the southern station of the array, K3, was placed at 4°11′N and K2 at 5°00′N. Stations K1 and K3 both carried an upward looking ADCP at 260-m depth to measure the near-surface currents with 8-m vertical resolution. The central mooring was equipped with rotor current meters at 144 m, 202 m, and 312 m. All moorings carried Aanderaa rotor current meters (RCMs) near 700 m and 1000 m, and at K2, deeper records were also obtained at 2035 m and 3543 m. The time interval of the ADCP and rotor current measure-

ments was 2 hours and 1–3 hours, respectively. The RCMs returned good data with only minor gaps or quality losses.

The ADCP on K3 yielded a perfect record with a closest near-surface level of good data of 30 m, due to side lobe interference of vertically traveling rays of the 20° inclined transducers. At station K1, some problems were encountered with the data quality of the ADCP, which at times emitted reduced energy, resulting in additional reduction of good data range. This loss in range resulted in an uppermost level of reasonable data quality at station K1 of 75 m, and some gappy information from 50-m depth. Deployment information on the three stations as well as annual means and standard deviations are shown in Table 1. Since for the purpose of this paper the tides and other high-frequency fluctuations are not of interest, the current-meter time series were low-pass filtered with a cutoff period of 40 hours. Current-vector time series of the low-passed currents are shown in Figures 2a–2c for stations K1–K3.

The first obvious result is that, except probably for the uppermost ADCP records at the nearshore station K1, a clear seasonal reversal, i.e., a dominant annual harmonic, in conjunction with the monsoon phases is not obvious. K1 currents show westward flow in both December to February phases for the upper 100 m (Figure 2a). In summer, the shallowest records show dominantly eastward currents during July and August, but already at 100 m the current alternated or was dominantly westward. The next station out, K2, with its top RCM at 144 m (Figure 2b), did not cover the shallow near-surface flow. The southern ADCP, at K3 (Figure 2c), similar to K1, showed a westward surface current during both winter monsoons, but the eastward currents in summer occurred earlier than at K1, already from early June to mid-July.
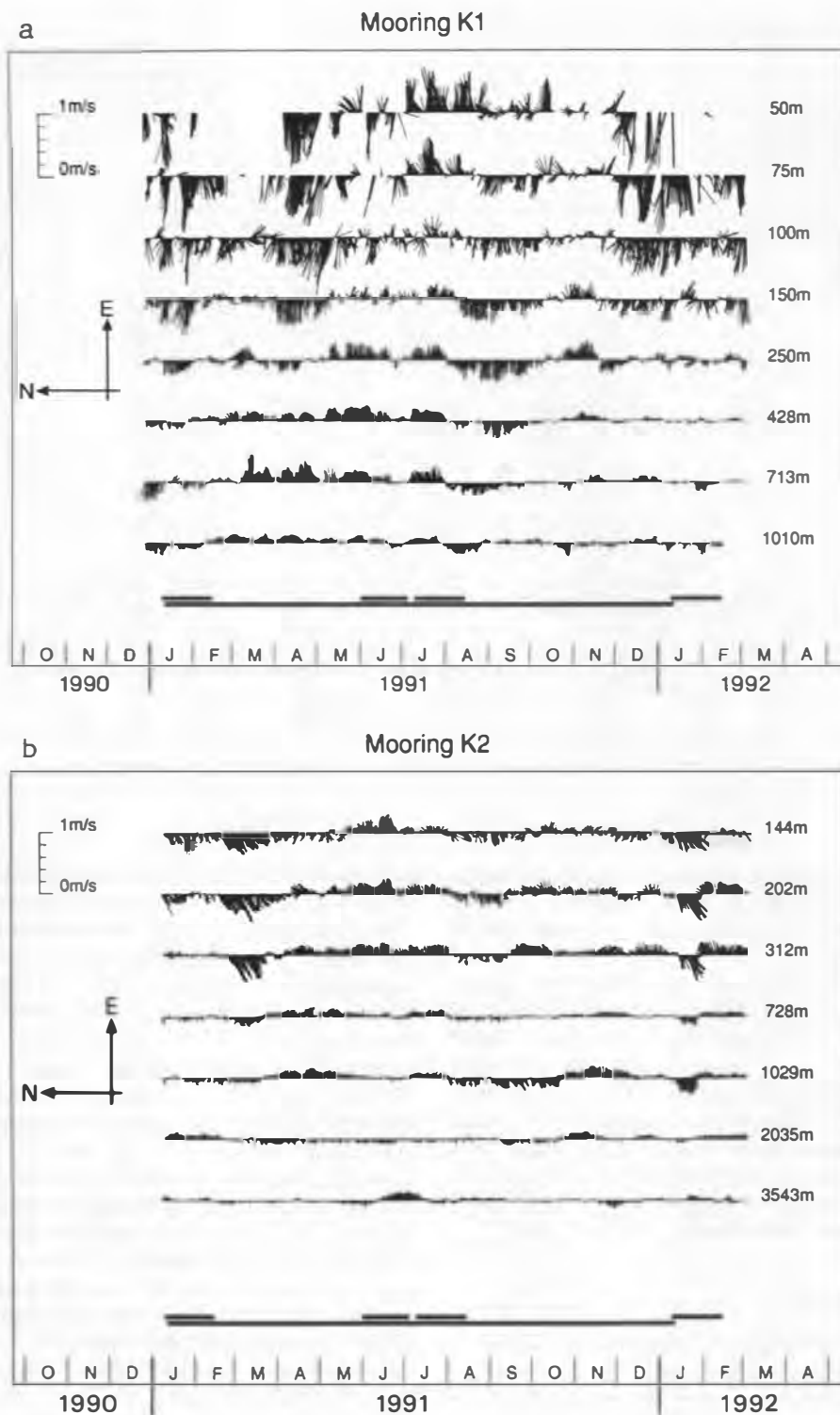
Figure 2. Forty-hour low-passed current-vector time series (upward = eastward) for stations (a) K1, (b) K2, and (c) K3. Averaging periods used for profiles in Figure 3 marked at bottom.

At all three stations, currents below 150 m were dominated by deep-reaching current reversals with periods of up to several months that are not in an obvious way correlated among the moorings. Yet, as shown below, the annual and semiannual harmonics together explain one third to one half of the zonal variance in much of the water column. An interesting finding is the upward phase propagation in the deep time series

that is quite obvious for some of the deep current fluctuations, e.g., during July/August at K1 and K3. Upward phase propagation was also observed along the equator earlier and is thought to be due to downward propagating energy of equatorial waves [*Luyten and Roemmich*, 1982].

For the presentation of means (Table 1), averages are taken over the first 12 months of the time series rather than
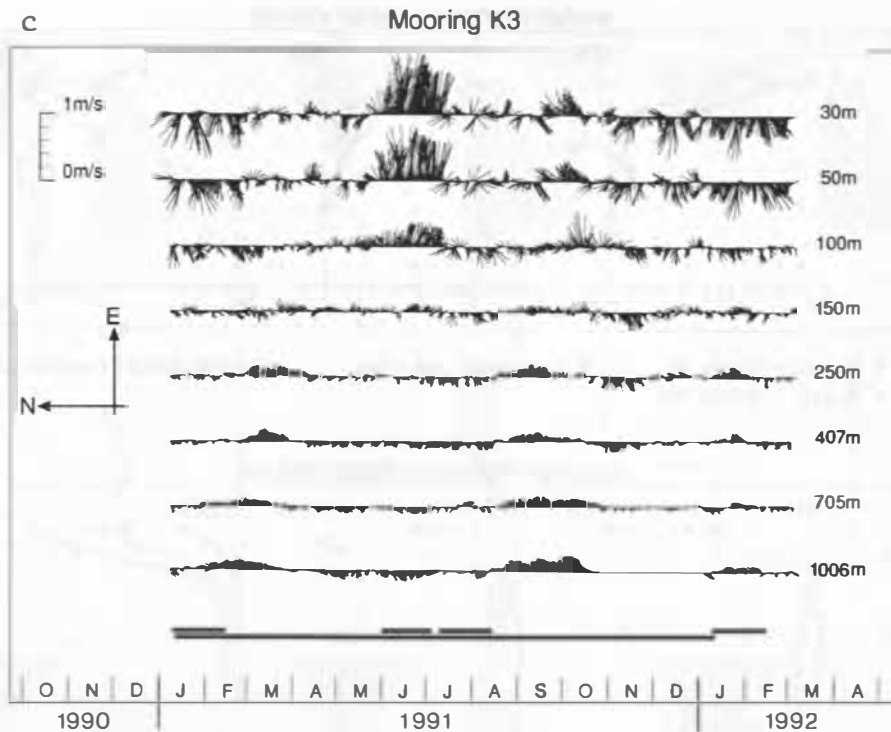
Figure 2. (continued)

over the entire 14-month deployment period to eliminate what seasonal signal there is, but the differences to record-length statistics are minor. The annual means of the zonal currents are weakly westward in the near-surface layer (Table 1) with maximum values at K1 near the coast, where unfortunately, the near-surface part of the ADCP profile was partly unreliable (see 50-m record, Figure 2a). Fluctuating kinetic energies (FKE; Table 1) that include the annual signal are >200 cm^2 s^{-2} in the near-surface layer and average 50 cm^2 s^{-2} at the 1000-m level. This level of deep variance is similar to that observed previously north of Madagascar at 12°S [*Schott et al.*, 1988], but lower than under the equatorial Somali Current where the average 4-year-long FKE was 130 cm^2 s^{-2} at the 1000-m level [*Schott et al.*, 1990].

Upper layer profiles of monsoon season means of the zonal current component for about month-long segments from both winter periods, January 10 to February 15, 1991 and 1992, are shown in Figure 3a. Currents are westward in both winters with large near-surface shears at both ADCP stations, decaying to <20 cm s^{-1} below 200 m and shoaling southward (Figure 3). As mentioned above, this shallow structure of the winter Monsoon Current means that the central mooring with its top rotor current meter at 144 m barely got into the bottom of the westward flow (Figure 3, middle graph). Shown for comparison are the profiles of the shipboard ADCP from R/V *Sonne* cruise SO73. They are averages from two legs of the cruise, December 27–29, 1990, and January 8–10, 1991, and from meridional intervals of 28-km width around each station. In this particular situation the flow is even shallower than for the monthly average.

The meridional extent of the westward surface current from late December 1990 to early January 1991 is apparent from the ADCP vector maps of Figures 4a and 4b. During the

southward leg of SO73 the southern limit of the current was sharply defined at 4°10′N, while on the northward return leg 2 weeks later, weaker westward flow extended southward to near 1°N. The currents at the 100-m level are either weak or not correlated with the surface flow (Figures 4d and 4e).

In the summer monsoon, the near-surface records of K1 and K3 show eastward flow at different time periods: June to mid-July at K3 and July to August at K1. The second period is associated with the fully established summer monsoon in the central Indian Ocean, while the May to June period is that of the semiannual equatorial jet. Profiles for both periods are presented in Figure 3b. For comparison, the shipboard ADCP profiles for July 28-30, 1993, are presented in Figure 3b, showing the current to decrease to near-zero values already above the 150-m level during the transect. The meridional extent of the current is indicated by the ADCP current vector map of Figure 4c. The interesting result there is that the Monsoon Current is separated from the coast by a 60-km-wide branch of westward flow, which is identifiable as Bay of Bengal water by its low salinities (D. Quadfasel, personal communication, 1993). The eastward flow regime extends from 2°40′N to 5°20′N, and is significantly decayed already at the 100-m level (Figure 4f). In 1991, station K1, which would be located in a westward branch like that of Figure 4c, did not record westward flow during most of July and August; instead it showed westward flow in June (Figure 2a), while currents further out were going eastward at the time (Figure 3c), resembling the situation found in the July 1993 ship survey.

Local winds along the 80°E line, latitudes 3°-6°N, for the deployment period (Florida State University (FSU), courtesy of M. Luther) are presented in Figure 5 as monthly mean pseudostress vectors. Eastward winds begin blowing in April with a maximum in June, at the time of the eastward
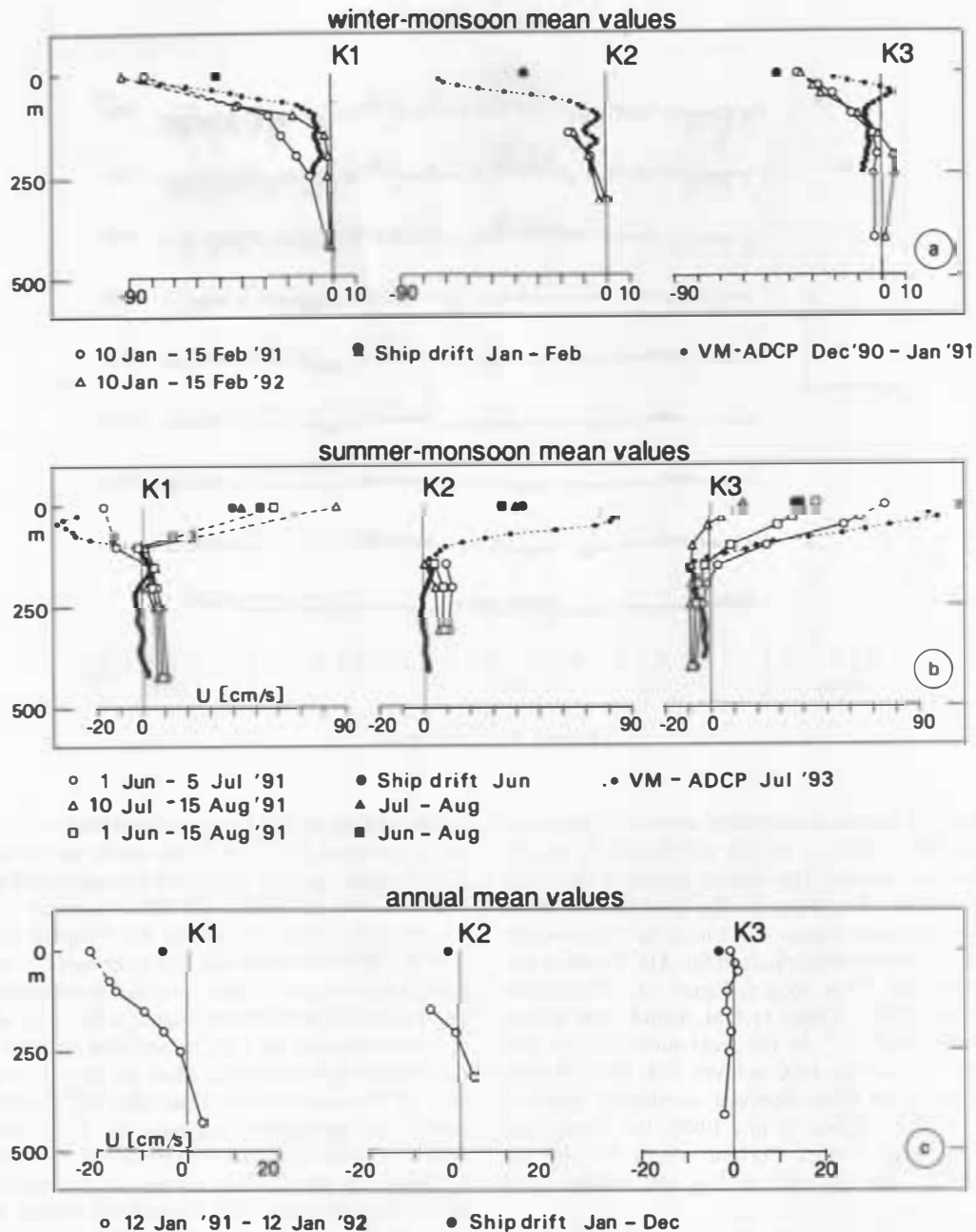
Figure 3. Averaged zonal velocities from moored instruments at stations K1, K2, and K3 in upper 500 m. (a) Two winter monsoon periods, January 10 to February 15 of 1991 and 1992. Also shown are shipboard ADCP profiles from SO73 survey, December 26, 1990 to January 9, 1991, and climatological ship drift currents for January/February. (b) Summer monsoon periods June 1 to July 5, July 10 to August 15, and June 1 to August 15, 1991. Also shown are shipboard ADCP profiles from SO88 survey and ship drifts for June and July/August. (c) Annual means, January 12, 1991, to January 12, 1992. Also shown are annual-mean ship drifts. Shipboard profiles are meridional averages over ±28 km around each mooring and for SO73 are averages over two cruise legs, December 26–31 and January 6–10. Ship drifts are from 5.5–6.0°N for K1, from 4.5–5.0°N for K2, and from 4.0–4.5°N for K3.

current burst at the offshore station. This eastward wind maximum in spring could be an extension of the semiannual eastward winds over the equator. A second eastward wind maximum occurs in September–October, again at the time of the semiannual eastward winds over the equator. Southwestward winds start blowing between November and December, with a stronger maximum in January 1992 compared to 1991.

3. Climatological Ship Drift Currents and Surface Extrapolation of Moored Currents

Ship drift current-vector distributions [*Cutler and Swallow*, 1984] show a western boundary current in the Bay of Bengal during November and December that appears to feed into a westward boundary current south of Sri Lanka. In the later part of the winter monsoon season, January and Febru-
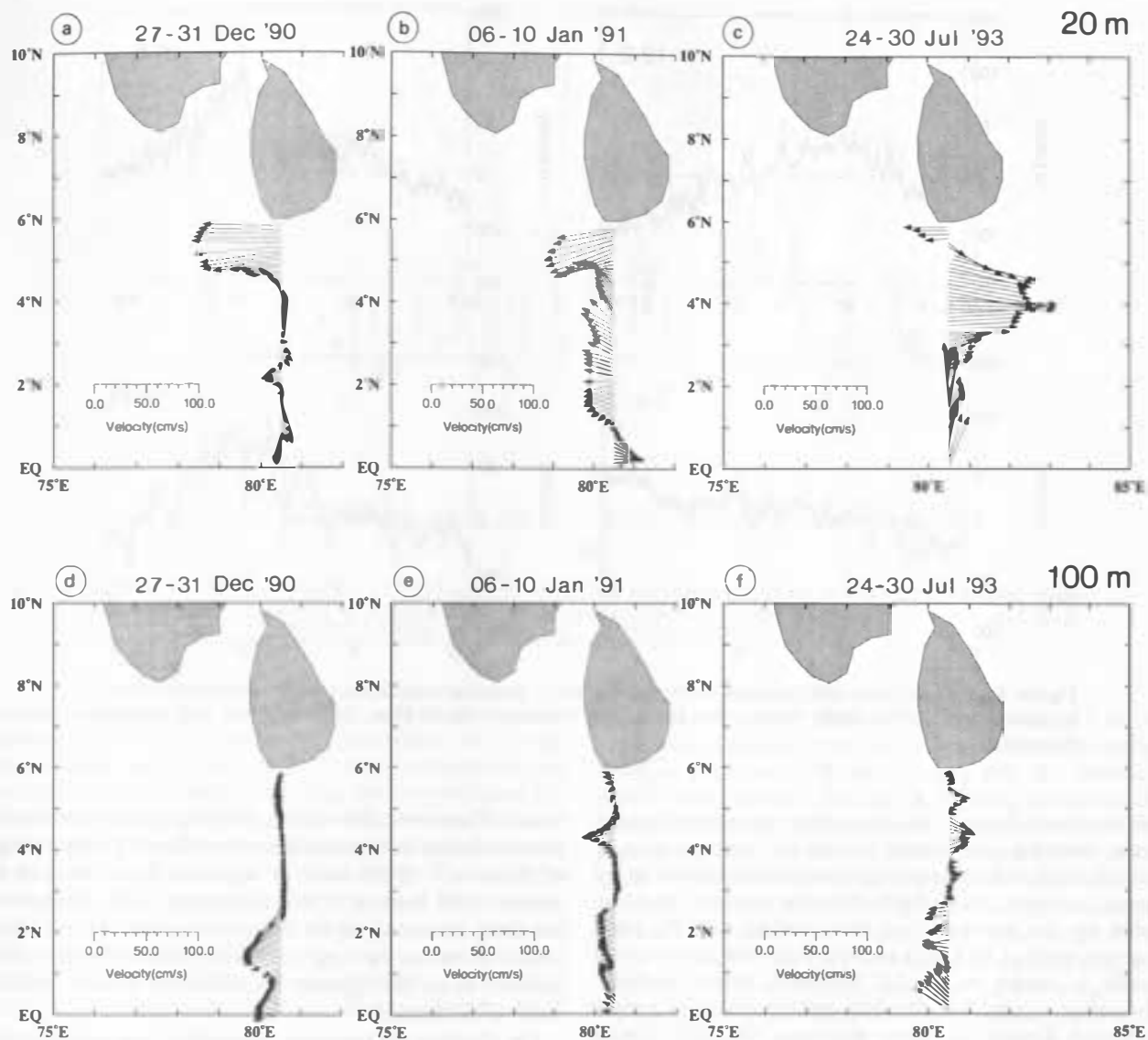
Figure 4. Current-vector plots of shipboard ADCP measurements between Sri Lankan coast and equator for 20-m and 100-m depth levels from (a and d) R/V *Sonne* cruise SO73, southward leg, December 27–31, 1990, and (b and e) northward leg, January 6–10, 1991, and (c and f) R/V *Sonne* cruise SO88, July 24–30, 1993.

ary, the flow, according to the ship drift currents, seems to originate more to the east, in the same latitude belt, rather than to come out of the western boundary current in the Bay of Bengal. During the summer monsoon, the ship drifts show southeastward flow along the west coast of India and eastward

flow in the 5°–10°N latitude belt east of Sri Lanka that merge with the eastward boundary current south of Sri Lanka.

Climatological averages of the zonal ship drift current components along 80°E and north of the equator are shown in Figure 6a. They were calculated for 3° longitude by 15'
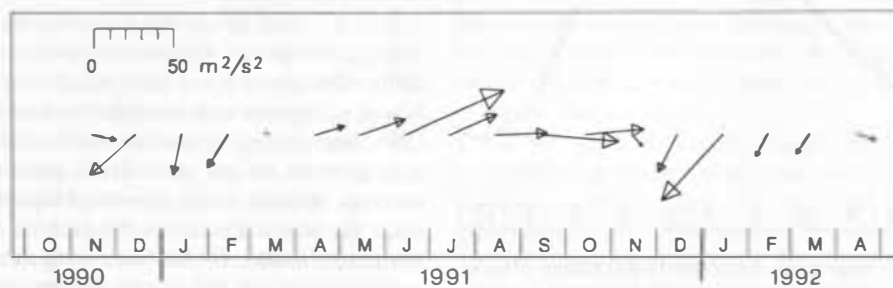

Figure 5. Monthly mean FSU pseudostress for November 1990 to April 1992 along 80°30'E, 3°–6°N.
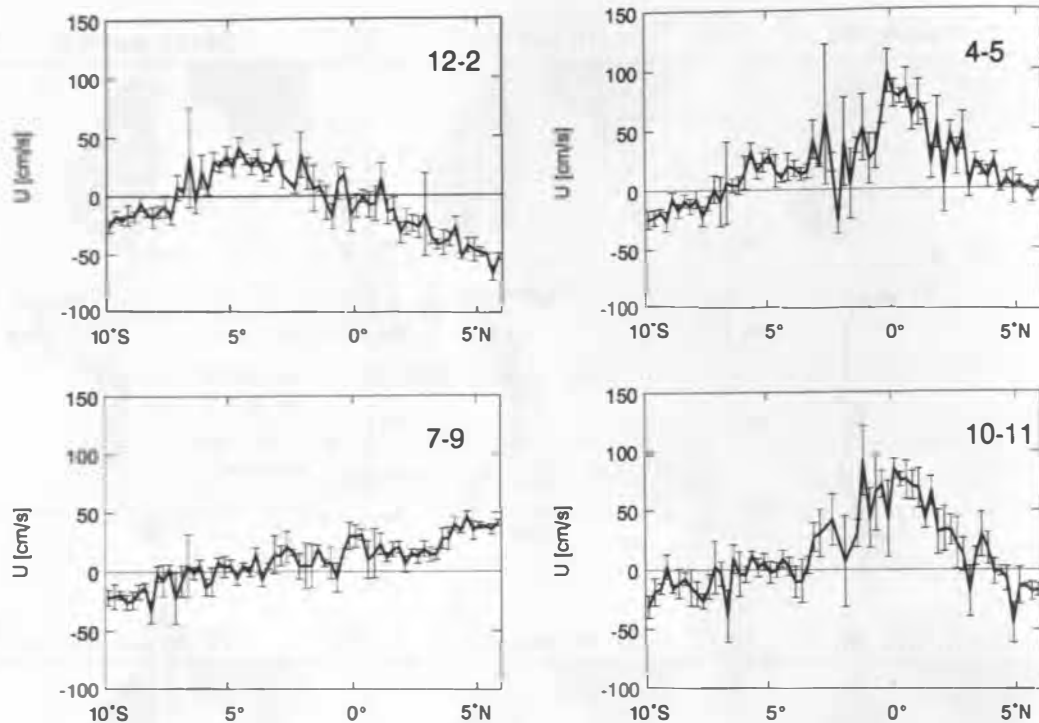
Figure 6a. Zonal ship drift currents (with mean errors), showing meridional profiles (calculated from 3° longitude by 0.25° latitude boxes) for December–February, April–May, July–August, and October–November.

latitude boxes. During July–September, the current is eastward, decaying only slowly toward the south, over a 3° latitude band, before increasing again on the equator. In the spring transition phase, April–May, the currents are dominated by the equatorial jet that reaches to 3°N, while currents south of Sri Lanka are near zero. The zonal current profile is similar in the fall transition phase, October–November, except that the flow past Sri Lanka is weakly westward. During the winter monsoon, the NMC has its westward maximum just off Sri Lanka, and reaches southward to about 2°N. The seasonal cycle of the zonal surface current from ship drifts over the center of our array, i.e., latitude range 5°15′–5°30′N (Figure 6b) shows a broad max-

Figure 6b. Zonal ship drift currents (with mean errors), showing monthly means of zonal component at 5°15′–5°30′N.

imum of eastward flow during July–September and maximum westward flow during December–January with a range of 90 cm s^{-1}. If the band of westward flow observed in summer 1993 north of 5°20′N (Figure 4c) is a consistently occurring feature during the summer monsoon, it is probably smoothed out by the large track averaging of the ship drift currents along the typically meridionally slanted courses south of Sri Lanka.

For checking the transport calculations, we will use ship drifts as surface currents for comparison with those estimated by extrapolating seasonal mean ADCP current profiles to the surface (Figure 3). Surface extrapolation at K3 is based on the 50-m- and 30-m-deep records. At K1 the 100-m- and 75-m-deep records had to be used, due to the reduced range of good ADCP data. For the winter 1992 monsoon that extrapolation would have lead at times to unrealistically high surface currents at K1 due to the low velocity at the 100-m level, which is a result of an extreme shallowness of the NMC during this time period compared with 1991. Therefore we used a surface value that was derived from the time series of extrapolated surface velocities at K1 with a threshold of 150 cm s^{-1}. For the winter monsoon means there is reasonable agreement of surface-extrapolated currents and ship drifts offshore, at K3 (Figure 3a), but shear extrapolation at K1, in agreement with the shipboard ADCP profiles of early 1991, leads to higher surface currents than ship drifts. The annual mean of the ship drifts agrees with the moored currents offshore in not showing a significant net flow either way, but also underscores the problem of shear extrapolation, in particular, for the fairly deep data (144 m and 202 m) at K2 (Figure 3c); this is why for the upper 150 m, only K1 and K3 were used for the transport calculations. The largest
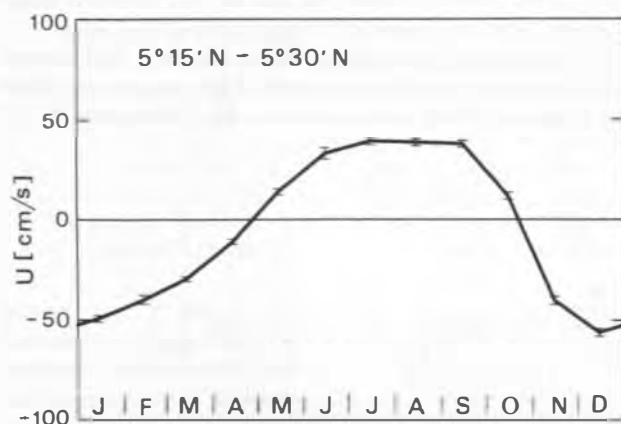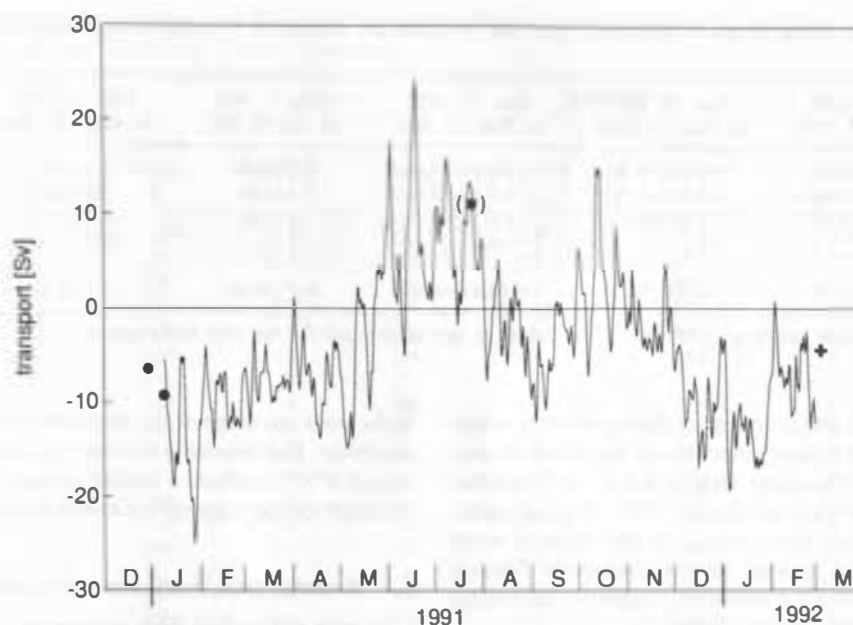
Figure 7. Times series of zonal transport in upper 300 m, calculated from moorings for latitude range 3°45'N–5°52'N, shipboard ADCP December 1990, January 1991 (solid circles), and July 1993 (solid circle within parentheses), and Pegasus March 1992 (cross); see text for details.

disagreement between both kinds of surface current averages occurs during the summer monsoon (Figure 3b). For the two different time periods in the summer monsoon the two surface current estimates show large deviations (Figure 3b). However, averaging the moored profiles from early June to mid-August 1991 yields a mean that shows a broad eastward flow, from K1 southward to K3, in good agreement with the ship drifts. This suggests that the position of the SMC may shift meridionally; it sometimes reached up to the coast and was sometimes separated from the coast by a coastal current regime of different origin. As discussed later, this feature may be associated with a reflected equatorial Rossby wave.

4. Transport Calculations

For the transport calculations from the levels below 150 m, we used a horizontal interpolation scheme that assumed the mean velocities of K1 to be representative from the shelf edge (5°52'E; Figure 1b) to the middle position between K1 and K2, corresponding to a segment width of 60 km. From there to halfway between K2 and K3 the K2 velocities were used, corresponding to a segment width of 82 km. From that midpoint to K3 and continuing the same distance to the south (to 3°45'N) the K3 values were used, corresponding to a segment width of 92 km.

For estimating the near-surface transports, two different methods were employed. One used the monthly mean ship drifts (Figure 6) for extrapolation to the surface; the other one, vertical shear extrapolation of the ADCP profiles at K1 and K3. Since an upward extrapolation at the central station from 203 m and 144 m would totally underestimate the surface current due to the instruments' being below the main current (Figures 3a and 3b), we used the values of the outer stations K1 and K3 for the surface currents north and south of K2. In the vertical, the mean velocities were then interpolated to 50-m intervals, down to 300 m, and transports were calculated for depth layers.

The constant northward extrapolation from K1 to the coast may introduce errors in the near-surface transports. While in December 1990 and January 1991 the shipboard ADCP measurements did not show much change of the meridional structure of the zonal flow just south of Sri Lanka, the current reversed direction near 5°20'N during summer 1993 (Figure 4). There might also be occasions when such shear occurred north of our northernmost station K1 and hence remained undetected by the array. South of the array, the ADCP current maps and the historical ship drift climatology (Figure 6) both show that the extrapolation of the K3 data to 3°45'N does not cover the total transport in both monsoon phases, and significant residual transports may remain.

A transport time series for the time period of January 1991 to February 1992, calculated by the shear extrapolation method, yields transport fluctuations in the range from 25 Sv westward to 24 Sv eastward (Figure 7) for the latitude range 3°45'–5°52'N. A phase of consistently eastward transport occurs during June–July, and transports are generally westward during both January–February observation periods. Shorter-period fluctuations with amplitudes of about 5 Sv are superimposed, for which, of course, the realism is questionable due to the coarse array resolution.

Table 2 and Figure 8 show the transports for depth increments for different averaging periods and for both vertical extrapolation methods. The calculated annual mean transports are 2–3 Sv to the west, i.e., not significantly different from zero.

For the winter monsoon average, the westward transport of the NMC down to 300-m depth was 12.8 Sv for the period January 10 to February 15, 1991, and 10.4 Sv during the equivalent period of 1992 when using shear extrapolation, and slightly lower when using the weaker climatological ship drifts (Figure 3a) as surface currents. Down to 100 m the transport is nearly the same in both years, and hence the

Table 2. Transports From Mean Velocities (Figure 3) for Different Monsoon Periods Using Shear Extrapolation and Ship Drift

Depth, m	Jan. 12, 1991 to Jan. 12, 1992	Jan. 10, 1991 to Feb. 15, 1991	Jan. 10, 1992 to Feb. 15, 1992	June 1, 1991 to July 5, 1991	July 10, 1991 to Aug. 15, 1991	June 1, 1991 to Aug. 15, 1991
0–50	−1.0 (−0.5)	−5.4 (−4.3)	−5.9 (−4.4)	3.7 (4.4)	3.7 (3.3)	4.7 (3.9)
50–100	−0.9 (−0.6)	−3.2 (−2.9)	−3.1 (−2.8)	2.1 (2.8)	0.9 (1.1)	2.0 (2.1)
100–200	−1.1 (−1.1)	−3.0 (−3.0)	−1.3 (−1.7)	1.4 (1.8)	−0.4 (−0.1)	0.6 (0.9)
200–300	−0.1	−1.2	−0.1	1.2	−0.1	0.5
0–300	−3.1 (−2.2)	−12.8 (−11.5)	−10.4 (−8.9)	8.4 (10.1)	4.1 (4.3)	7.8 (7.5)

All values are in units of sverdrups ($=10^6$ m^3 s^{-1}). Values in parentheses are for the ship drift method.

difference to the 0- to 300-m transport during the first winter monsoon arises from higher velocities in the lower layers. The shipboard ADCP sections yielded 6.4 Sv in December 1990 and 9.2 Sv westward in January 1991, in good agreement with the moored time series. At the time of array retrieval, a somewhat coarser section repeat by Pegasus profiling resulted in 4.4 Sv westward, again in reasonable agreement with the time series (Figure 7).

For the summer monsoon of 1991, Table 2 shows the transports for the periods distinguished in the previous sections, i.e., the period of strong eastward currents at K3 (June 1 to July 5), and the subsequent period of eastward currents at K1 (July 10 to August 15). For the first period the shear-extrapolated transport above 300 m was 8.4 Sv to the east, but stronger with the ship drifts used, which were higher during this period at both K1 and K3 than the shear-extrapolated surface currents. For the second period the subsurface counterflow (Figure 8) decreased the eastward transport to about 4 Sv. This countercurrent appeared at the end of July at the 1000-m level at K1 and reached, with an upward phase propagation, the 100-m level in mid-August (Figure 2a), reducing even the zonal velocities at the 50-m level. The total transport for the period June 1 to August 15 above 300 m was 7.8 Sv from shear extrapolation, in good agreement with ship drift extrapolation.

The shipboard ADCP measurements in 1993 (Figure 4c) for the situation similar to the June period of the moored data, i.e., when the current maximum was located near Sri Lanka, resulted in an eastward transport of 11.1 Sv above 300 m for the array domain (Figure 7) and 15 Sv north of 2°N. The contribution of 4 Sv to the SMC from south of our array, i.e., between 3°45′N and 2°N, as obtained by the shipboard ADCP, may serve as an estimate of the transport error due

to the poor coverage of the monsoon current with only three moorings. Extrapolating the current profile at K3 linearly to zero at 2°N would add a similar amount (2.6 Sv) to the array transport of the summer monsoon period.

5. Annual and Semiannual Components

Despite the visibly high content of shorter than semiannual variability in the current records, about one third to half of the variance of the zonal currents recorded during 1991/1992 with the moored instruments is explained by the annual and semiannual harmonics (Table 3). Near-surface records of the zonal current component that entered into the transport calculations are shown in Figure 9a, with the composite of the first two harmonics superimposed. The annual harmonic amplitude at 50-m depth is about 20 cm s^{-1} at K1, and the phase of the maximum advances from mid-July near the coast to about a month earlier at the southernmost station. This phase difference is not significant, though, given the phase errors of typically 30–50° of the harmonic fits. At the deeper levels, down to 2000 m, the amount explained is similarly as high as or partly even higher than in the near-surface layer with mean annual and semiannual amplitudes of 5.4 and 5.5 cm s^{-1}, respectively, when averaged for the 400- to 2000-m range. As mentioned above, these deep variations and their possible physical causes will be addressed in a different paper, together with near-equatorial observations.

The annual harmonic transport amplitude (Figure 9a) is 7.1 Sv, and the corresponding phase of the eastward maximum is in July. The semiannual signal is 2.1 Sv with its eastward maxima in early June and early December, i.e., 1 month after the maximum of the semiannual equatorial jet. Both
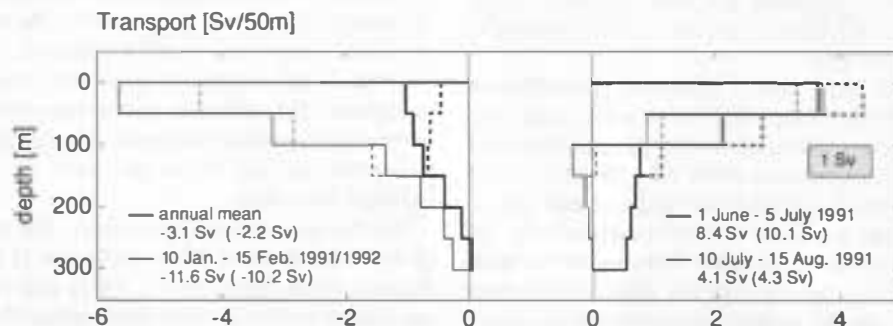
Transport [Sv/50m]

Figure 8. Transports for shear extrapolation (solid lines) and ship drifts (dashed lines) as surface currents: for the annual mean (January–January), a mean of the two winter monsoon phases on the left and for the two summer monsoon phases on the right.

Table 3. Amplitudes and Phases of Annual and Semiannual Components in Zonal Currents and Monsoon Current Transport

Mooring	Record Depth, m	Annual		Semiannual		Fraction of Variance Explained
		Amplitude, cm s^{-1}	Phase (Jan. 1)	Amplitude, cm s^{-1}	Phase (Jan. 1 and July 1)	
K1	75*	23.3*	236*	3.7*	74*	0.33*
	100	10.5	239	3.6	58	0.13
	200	4.1	130	8.2	307	0.17
	428	8.8	119	6.3	287	0.49
	713	10.5	116	6.4	246	0.46
	1010	5.7	119	3.8	210	0.34
K2	144	7.4	210	6.3	300	0.42
	202	5.6	200	7.1	294	0.28
	312	3.1	224	6.9	297	0.22
	728	2.4	138	3.9	276	0.31
	1029	4.3	96	6.8	282	0.39
	2035	3.9	344	1.9	26	0.44
	3543	1.2	210	2.1	50	0.17
K3	30	26.8	186	9.0	308	0.50
	50	20.6	183	9.6	306	0.43
	100	8.8	179	6.3	287	0.33
	200	1.4	71	3.4	147	0.11
	407	2.2	334	6.0	142	0.34
	705	4.1	292	6.3	142	0.52
	1006	6.7	304	8.4	141	0.66
Ship drifts (5°–5.5°N)		49.7	199	8.0	134	0.97
Transport		7.1 Sv	206	2.1 Sv	302	0.50

*Gappy record.

harmonics superimpose for an overall maximum in early summer and explain half the moored transport variance.

Harmonics for the ship drift currents are presented in Figure 9b. While the annual amplitude falls off from >50 cm s^{-1} near the Sri Lankan coast to <20 cm s^{-1} north of the equator, the semiannual amplitude falls from about 40 cm s^{-1} near the equator to values <10 cm s^{-1} near Sri Lanka. The annual harmonic in the ship drifts has its maximum in July, in agreement with the near-surface mooring results; the phase advances only slightly toward the equator, suggesting that the difference between the two current-meter stations is due to aliasing by the mesoscale variability rather than a representation of reality.

The semiannual ship drift harmonic has its maximum in April (and October) near the equator, representing the semiannual equatorial jet, and shifts by about 1 month toward Sri Lanka. This is not in agreement with the results from the moored stations (Table 3). The reason for this discrepancy may be the meandering of the SMC, which makes it appear at K1 and K3 at different times (Figure 2). This meandering when aliased by poor array resolution, can result in an artificially increased second harmonic (Figure 9a). This may explain the high amplitudes of the semiannual harmonics relative to the annual harmonics (Table 3), which cannot be seen in the ship drifts at this latitude (Figure 9b), and the phase difference of the semiannual harmonic against the equatorial jet.

6. Discussion

We have described results of moored array current measurements in the Monsoon Current south of Sri Lanka that revealed an extreme shallowness of the current. With typical deep-water subsurface rotor current-meter moorings, this flow would in its major part not have been covered. Even with upward looking ADCPs, as used here on two of the three moorings, the near-surface data loss due to surface backscatter and the strong near-surface shears required upward extrapolation based on the shears in the good data range. Using these current time series, we estimated a transport time series for the latitude band between 3°45'N and the coast of Sri Lanka.

During the two winter monsoons covered, the flow was westward as expected, with mean transports of 12 and 10 Sv in 1991 and 1992, respectively. The situation was more variable during the summer monsoon: the mooring next to the northern boundary shows a different phase of persistent eastward flow than the southernmost mooring. A shipboard ADCP survey in July 1993 even showed a zone of westward flow just south of Sri Lanka, carrying low-salinity waters out of the Bay of Bengal, a situation in qualitative agreement with what the moorings showed during June 1991: westward flow at the northernmost station, K1, and eastward flow further south (Figure 3b). Averaging over the entire period of the southwest monsoon (June 1 to August 15) yielded a transport of 8 Sv. Some confidence in the seasonal transport numbers obtained could be taken from the fact that surface extrapolation by the shears as measured by the ADCPs yielded values rather similar to when climatological ship drifts were used as surface currents.

The transport derived from the array is not total Monsoon Current transport, since the flow extends southward, beyond the regime covered by the moored array. Climatological ship
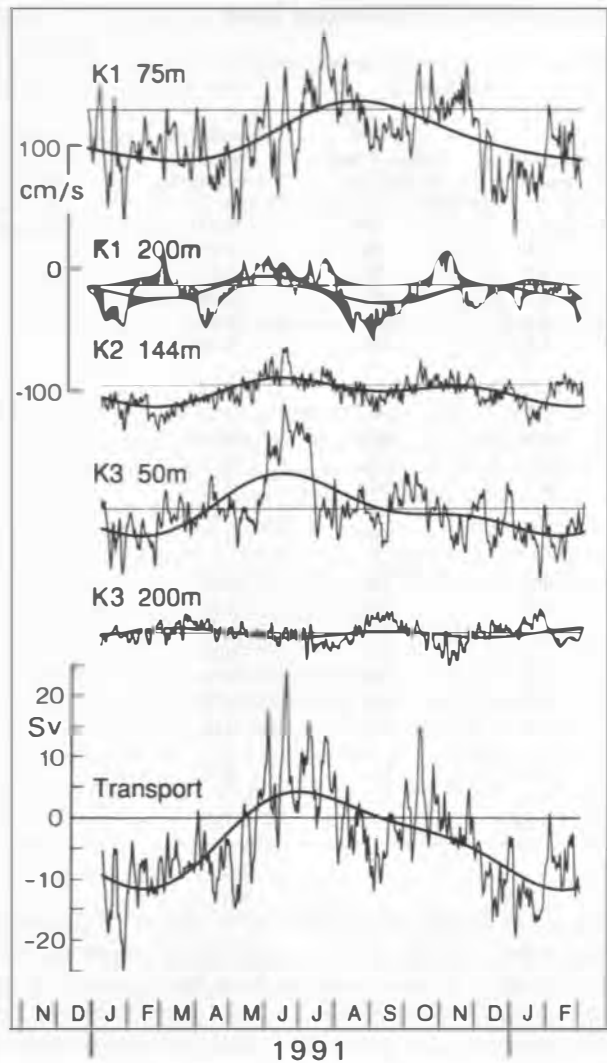
Figure 9a. Zonal velocity components of selected near-surface records from stations K1, K2, and K3 and transport time series (bottom graph) with annual plus semiannual harmonics superimposed.
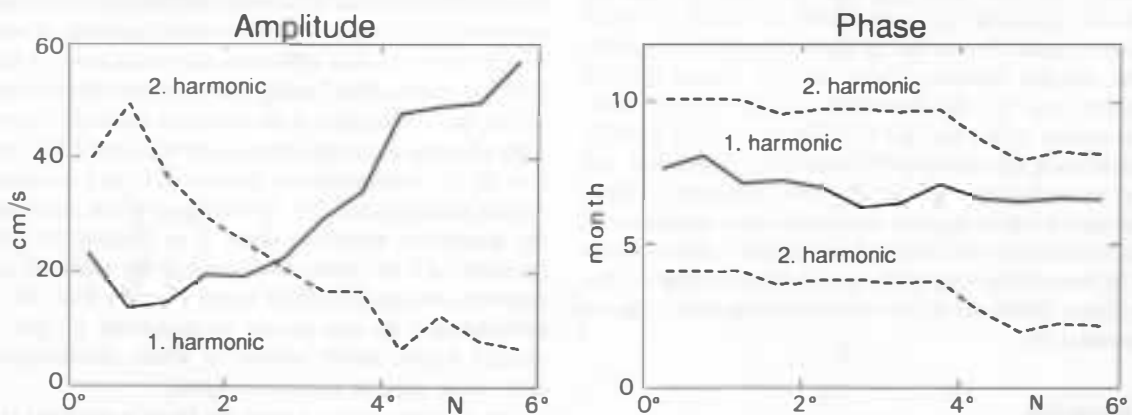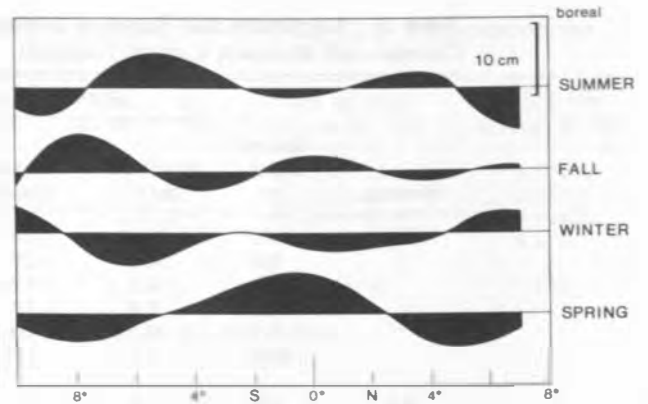

Figure 10. Meridional profiles of mean seasonal sea surface height anomalies in 75°–80°E longitude belt for (from top) summer, fall, winter, and spring (reprinted from *Scharrel* [1990]) (also A. Scharrel, personal communication, 1993).

drifts show eastward surface currents across 80°E everywhere north of the equator during the summer monsoon, although weak south of 3°N; and westward currents north of about 2°N during the winter monsoon (Figure 6a). Another view at the meridional extent of the Monsoon Current can be obtained from Geosat altimetry surface height variations, as analyzed by *Scharrel* [1990] for the longitude range 75°–80°E (Figure 10). The height anomalies show the equatorial jet in spring and somewhat weaker, in fall with surface slopes reaching northward to near 4°N. Winter monsoon surface slopes indicate westward geostrophic flow of the NMC north of 2°–3°N, while the geostrophic flow of the SMC appears to be restricted to a narrower latitude range, north of about 4°N.

Our own shipboard ADCP section of July 1993 (Figure 4c) yielded, in addition to 11 Sv eastward in the array domain, an incremental transport of 4 Sv in the latitude range between the array and 2°N, a value similar to that obtained by extrapolating the SMC array transport southward to 2°N. In one of the winter monsoon ADCP sections (Figure 4b) there was also an extension southward, amounting to 3.8 Sv between the array and 2°N.

Figure 9b. Amplitudes and phases of annual and semiannual harmonics for zonal ship drift velocities along 80°E, latitude range 0°-6°N.

When comparing altimetry sea surface height (SSH) anomalies with ship drift currents, it must be taken into consideration that the ship drifts include Ekman currents while surface slopes do not. The wider band of zonal surface currents in both monsoon seasons in the climatological ship drifts (Figure 6a) south of the immediate boundary regime compared to satellite SSH anomalies can partly be explained as Ekman flow, although Ekman transports across 80°E for the region between the southern array limit and 2°N are fairly weak compared to overall Monsoon Current transports. For the *Hellerman and Rosenstein* [1983] climatology, they amount only to about 1.0 Sv westward in December–January and 0.5 Sv eastward during June–August; for the FSU pseudostress time series during our deployment (Figure 5), that transport (using a drag coefficient of 1.3×10^{-3}) for the summer monsoon of 1991 dropped from 1.1 Sv in June to near zero in August and had a winter monsoon maximum of 1.6 Sv westward during January 1992.

Some insight into the spatial structure of the flow in the Monsoon Current regime has been gained recently from numerical models of the Indian Ocean, and we review in the following some of these results in the light of our findings. Since these models reproduced salient features of the monsoon-driven circulation quite well in regions where sufficient observations exist, e.g., on the equator or in the Somali Current regime, they may serve as guidelines for those regions of which little is known, particularly with respect to the subsurface circulation. The fact that most of the models are driven by the *Hellermann and Rosenstein* [1983] wind stress climatology makes their intercomparison independent of driving force differences.

The primitive equation model of the Geophysical Fluid Dynamics Laboratory (GFDL), Princeton, N. J., that was developed for the Indian Ocean north of 30°S (G. Philander, personal communication, 1988), and is dynamically similar to the tropical Atlantic model of *Philander and Pacanowski* [1986], was found to represent the seasonal cycle of the near-equatorial circulation quite well, at least in the western part of the basin [e.g., *Schott*, 1986; *Visbeck and Schott*, 1992]. In that model, the Monsoon Current south of the island of Sri Lanka is confined to the upper 200 m and the region north of 3°N and shows a seasonal reversal (Figure 11).

The transport in the upper 150 m of the GFDL model is eastward during the summer monsoon and westward in the winter monsoon with a transport amplitude of 11 Sv. The supply of water for the eastward boundary current off Sri Lanka during the summer monsoon stems from waters to the west in the same latitude belt, and does not come from the northwest, from the Arabian Sea, or as a boundary current along the west coast of India. The eastward flow has its high-speed core offshore and reaches southward to 2°N, similar to the summer 1993 ship observations. It is separated from eastward equatorial flow by only a narrow regime of weak westward currents (Figure 11d). Below 100 m, the flow in the GFDL model reverses in the summer monsoon to form a westward countercurrent in the latitude range north of 2°N. During the winter monsoon (Figure 11a), the westward flow draws mostly from waters in the 3°–8°N latitude belt rather than from the Bay of Bengal. It decays southward to 2°N, but merges in February in the south with a westward equatorial flow regime, making the surface distinction of both currents difficult (Figure 11b).
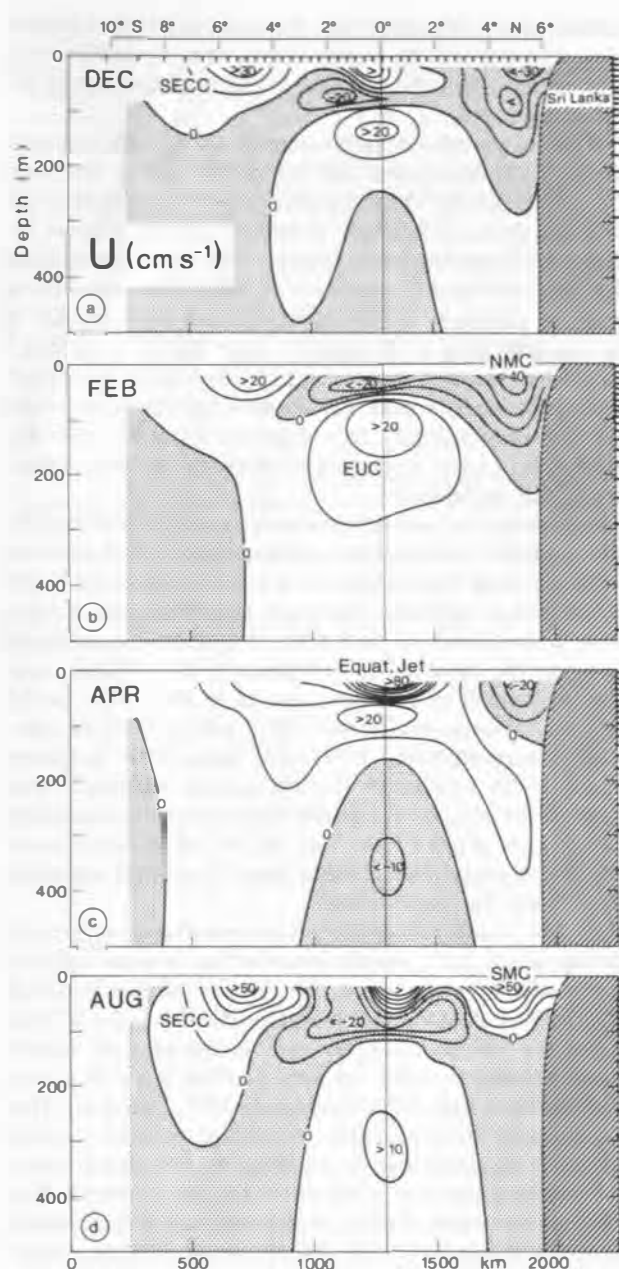

Figure 11. Zonal current distribution along the 80°E section in the GFDL model for (a) December, (b) February, (c) April, and (d) August.

In the global primitive equation model of *Semtner and Chervin* [1992] (also B. Semtner, personal communication, 1991), the island of Sri Lanka is merged with the Indian subcontinent, and the southern extent of the topography there is located at 8°N rather than 6°N as in the real ocean. This is interesting by comparison with other models in the context of the potential existence of an open-ocean eastward jet south of Sri Lanka rather than a northern coastal boundary current. During the summer monsoon, that model does indeed show an eastward current core that is detached from the northern coast, centered at 5°N and reaching down to 200 m. This eastward flow apparently also draws from water to the west at the same latitude and not from the north at the Indian coast, similar to the GFDL model. The eastward

current core is separated from the coast at 8°N by a branch of westward flow. This westward flow along the Indian coast is there throughout the year and has its maximum during the winter monsoon.

While in general circulation models (GCMs) the physical relations between cause and effect are mostly obscured through their complexity, insights about the mechanisms of monsoon-driven circulation variability can be obtained by dynamically simpler layer models. This has recently been demonstrated by *McCreary et al.* [1993], who carried out a series of sensitivity studies to understand the dynamics of the monsoon circulation using a $2\frac{1}{2}$-layer model. Their study shows that remote forcing by equatorially trapped waves and remote forcing by coastal Kelvin waves can both be important for understanding the Monsoon Current variability south of Sri Lanka. Some specific results concerning remote forcing are as follows.

1. During the summer monsoon, an equatorial Rossby wave radiates westward as a consequence of Kelvin wave reflection from the Indonesian coast associated with the intermonsoon eastward equatorial jet. When the Rossby wave arrives south of Sri Lanka, it weakens the eastward flow near the equator but strengthens it on its flanks, near 5°N. In their fit of equatorial waves to the GFDL model currents, *Visbeck and Schott* [1992] and M. Visbeck (personal communication, 1993) also found this dominant Rossby wave responsible for the general westward flow north of the equator in summer underneath the immediate Ekman layer (Figure 11d). Thus the arrival of such a wave could be an explanation of the apparent meridional migration of the SMC that we observed.

2. The model underscores the importance of remote forcing effects in the eastern Arabian Sea. In a test calculation in which the winds over the Arabian Sea are switched off in the model, model currents along the west coast of India during the SW monsoon are still southward, and Rossby wave radiation into the southern Arabian Sea still occurs from the tip of India [*McCreary et al.*, 1993, Figure 6a]. This test suggests the importance of coupling between the two basins via coastal Kelvin waves along the Sri Lankan coast. It provides a possible explanation for the westward flow observed just south of Sri Lanka during part of the summer monsoon, if this flow were indeed a regular summer monsoon phenomenon.

3. Similarly, in the winter monsoon, model currents off western India are mainly remotely driven via coastal Kelvin waves generated by the collapse of the SW monsoon winds over the Bay of Bengal in the previous fall. These currents subsequently propagate as Rossby waves into the central Arabian Sea.

From the above, one might conclude that breaks in the monsoon over the Bay of Bengal could sporadically generate coastal Kelvin waves at any time during the summer monsoon. These waves could then propagate around Sri Lanka to cause sporadic bands of westward flow south of the coast as observed by us during the summer monsoon. They could also contribute to the different conditions observed off SW India at particular times of a summer monsoon. While *Shetye et al.* [1990] found southward surface flow with a northward undercurrent in June 1987, we observed weak northward near-surface currents off India along the 8°N section of *Sonne* cruise SO89 in August 1993 with a subsurface core at about 100 m.

Further, the results summarized above make one wonder how realistic the GFDL and similar GCMs really are in representing the composition and sources of the Monsoon Current flow south of India/Sri Lanka. Their grid spacing is not good enough to be able to cope with baroclinic coastally trapped waves. Further, the meridional shape of a boundary current south of Sri Lanka in such models depends very much on their friction parameterization. Hence, the predominance of a reversing low-latitude zonal flow in these models and lack of boundary linkage between the Bay of Bengal and Arabian Sea may be more an artifact of those models rather than a representation of reality.

Issues to be addressed in a further study are the kinematics and dynamics of the deep variations of several cm s^{-1} amplitude seen in the moored currents for which the annual and semiannual harmonics contributed a significant part of the total variance, suggesting driving by the annually reversing monsoon winds and the semiannual zonal winds along the equator. The upward phase propagation observed during the summer monsoon in our moored array data is a phenomenon already observed by other investigators earlier in the context of the semiannual equatorial variability [*McPhaden*, 1982; *Luyten and Roemmich*, 1982] in the central equatorial Indian Ocean. It indicates the presence of downward propagating free waves. The deep annual and semiannual variations in the seasonally driven GFDL model for the area around 5°N, 80°E had amplitudes comparable to those observed, and as shown by *Visbeck and Schott* [1992], the deep variability in that model could to a large degree be explained by a superposition of equatorial Kelvin and Rossby waves. An extension southward of the moored array along 80°E, from 5°N to across the equator, that was deployed in summer 1993 is anticipated to provide additional evidence regarding the role of equatorial waves in the Monsoon Current variability.

References

Cutler, A. N., and J. C. Swallow, Surface currents of the Indian Ocean (to 25°S, 100°E), *IOS Tech. Rep. 187*, Inst. of Oceanogr. Sci., Wormley, England, 1984.

Hellermann, S., and M. Rosenstein, Normal monthly wind stress over the world ocean with error estimates, *J. Phys. Oceanogr.*, *13*, 1093–1105, 1983.

Luyten, J. R., and D. H. Roemmich, Equatorial currents at semiannual period in the Indian Ocean, *J. Phys. Oceanogr.*, *12*, 406–413, 1982.

McCreary, J. P., P. K. Kundu, and R. L. Molinari, A numerical investigation of dynamics, thermodynamics and mixed-layer processes in the Indian Ocean, *Prog. Oceanogr.*, *31*, 181–244, 1993.

McPhaden, M. J.. Variability in the central equatorial Indian Ocean, Part I, Ocean dynamics, *J. Mar. Res.*, *40*, 157–176, 1982.

Philander, S. H., and R. C. Pacanowski, A model of the seasonal

cycle in the tropical Atlantic Ocean, *J. Geophys. Res.*, *91*, 14,192–14,206, 1986.

Potemra, J. T., M. E. Luther, and J. J. O'Brien, The seasonal circulation of the upper ocean in the Bay of Bengal, *J. Geophys. Res.*, *96*(C7), 12,667–12,683, 1991.

Rao, R. R., R. L. Molinari, and J. F. Festa, Evolution of the climatological near surface thermal structure of the tropical Indian Ocean, 1, Description of mean monthly mixed layer depth, and sea surface temperature, surface current, and surface meteorological fields, *J. Geophys. Res.*, *94*(C8), 10,801–10,815, 1989.

Reverdin, G., The upper equatorial Indian Ocean: The climatological seasonal cycle, *J. Phys. Oceanogr.*, *17*, 903–927, 1987.

Scharrel, A., Geosat-Altimetrie im Indischen Ozean auf zwei Meridionalschnitten entlang 79°E und 65°E, Diploma thesis, 97 pp., Univ. Kiel, Kiel, Germany, 1990.

Schott, F., Seasonal variation of cross-equatorial flow in the Somali Current, *J. Geophys. Res.*, *91*, 10,581–10,584, 1986.

Schott, F., M. Fieux, J. Kindle, J. Swallow, and R. Zantopp, The boundary currents east and north of Madagascar, 2, Direct measurements and model comparisons, *J. Geophys. Res.*, *93*, 4963–4974, 1988.

Schott, F., J. C. Swallow, and M. Fieux, The Somali Current at the equator: Annual cycle of currents and transports in the upper 1000 m and connection to neighboring latitudes, *Deep Sea Res.*, *37*, 1825–1848, 1990.

Semtner, A., Jr., and R. M. Chervin, Ocean general circulation from a global eddy-resolving model, *J. Geophys. Res.*, *97*(C4), 5493–5550, 1992.

Shetye, S. R., A. D. Gouveia, S. S. C. Shenoi, D. Sundar, G. S. Michael, A. M. Almeida, and K. Santanam, Hydrography and circulation off the west coast of India during the Southwest Monsoon 1987, *J. Mar. Res.*, *48*, 359–378, 1990.

Visbeck, M., and F. Schott, Analysis of seasonal current variation in the western equatorial Indian Ocean: Direct measurements and GFDL model comparison, *J. Phys. Oceanogr.*, *22*, 1112–1128, 1992.

Woodberry, K. E., M. E. Luther, and J. J. O'Brien, The wind-driven seasonal circulation in the southern Indian Ocean, *J. Geophys. Res.*, *94*(C12), 17,985–18,002, 1989.

Wyrtki, K., *Oceanographic Atlas of the International Indian Ocean Expedition*, 531 pp., National Science Foundation, Washington, D. C., 1971.

Wyrtki, K., An equatorial jet in the Indian Ocean, *Science*, *181*, 262–264, 1973.

J. Fischer, J. Reppin, and F. Schott, Institut für Meereskunde, Universität Kiel, Düsternbrooker Weg 20, 24105 Kiel, Germany.

D. Quadfasel, Institut für Meereskunde, Universität Hamburg, Troplowitzstrasse 7, 22529 Hamburg, Germany.